

A simple vision-based fall detection technique for indoor video surveillance

Jia-Luen Chua · Yoong Choon Chang ·
Wee Keong Lim

Received: 8 October 2012 / Revised: 29 April 2013 / Accepted: 29 April 2013 / Published online: 21 May 2013
© Springer-Verlag London 2013

Abstract Falls are one of the major health hazards among the aging population aged 65 and above, which could potentially result in a significant hindrance to their independent living. With the advances in medical science in the last few decades, the aging population increases every year, and thus, fall detection system at home is increasingly important. This paper presents a new vision-based fall detection technique that is based on human shape variation where only three points are used to represent a person instead of the conventional ellipse or bounding box. Falls are detected by analyzing the shape change of the human silhouette through the features extracted from the three points. Experiment results show that in comparison with the conventional ellipse and bounding box techniques, the proposed three point-based technique increases the fall detection rate without increasing the computational complexity.

Keywords Fall detection · Analysis of human shape variation · computer vision

List of Symbols

H	Height of the bounding box
W	Width of the bounding box
h_{R1}	Height of region $R1$
h_{R2}	Height of region $R2$
h_{R3}	Height of region $R3$

w_{R1}	Width of region $R1$
w_{R2}	Width of region $R2$
w_{R3}	Width of region $R3$
(g_{R1x}, g_{R1y})	Centroid coordinate of region $R1$
(g_{R2x}, g_{R2y})	Centroid coordinate of region $R2$
(g_{R3x}, g_{R3y})	Centroid coordinate of region $R3$
$D1$	Distance between $P1$ and $P2$
$D2$	Distance between $P2$ and $P3$
θ_1	Orientation of the line formed by $P1$ and $P2$
θ_2	Orientation of the line formed by $P2$ and $P3$
p	Ratio of the distance $D1$ over $D2$
p_{t-1}	Ratio of the distance at previous frame
p_t	Ratio of the distance at current frame
θ_r	Reference angle
D_r	Length reference
θ_{N1}	Orientation of the line formed by $P1$ and $P2$ at the 10th frame after a possible fall
θ_{N2}	Orientation of the line formed by $P2$ and $P3$ at the 10th frame after a possible fall
θ_{D1}	Orientation difference between θ_{N1} and θ_r
θ_{D2}	Orientation difference between θ_{N2} and θ_r
μ_θ	Mean of the two orientation differences, θ_{D1} and θ_{D2}
D_{diff}	Change in sum of the length of the lines after a possible fall

J.-L. Chua (✉) · Y. C. Chang · W. K. Lim
Faculty of Engineering, Multimedia University, Cyberjaya, Malaysia
e-mail: chua.jia.luen11@student.mmu.edu.my

Y. C. Chang
e-mail: ycchang@mmu.edu.my

W. K. Lim
e-mail: wklm@mmu.edu.my

1 Introduction

Falling among the elderly has always been an important healthcare issue. Each year, one in every three adults aged 65 years and above falls [1]. In Malaysia, population aged 65 and above has increased from 4.3 % in 2007 to 4.5 % in 2009

and the elderly population is expected to increase to 7% by 2020 [2,3]. As in other Western countries, this population grows at a larger rate each year [4]. Since majority of the elderly population live in private house, falls can be a major risk for those who live alone as injuries from a fall can be life threatening. Report shows that 2.2 million nonfatal fall injuries among older adults in United States of America were treated in emergency departments and more than 581,000 of these patients were hospitalized in 2009 [5]. A serious fall at home may lead to the risk of death or “post-fall syndrome” if the person cannot call for help immediately after a fall. In light of this, development of fall detection system has gained attention in recent years as this system can alert paramedic personnel in time after a fall has occurred in order to prevent post-fall consequences and save the life of the elderly.

Fall detection systems available in the market are mostly worn-sensor based [6,7], which are basically electronic devices whereby the elderly need to wear or put in the pocket. These wearable fall detectors normally use accelerometer or manual help button as the sensor to detect a fall. However, these wearable fall detectors have a few drawbacks. One of the weaknesses for such detectors is that the elderly people may forget to wear them and help buttons are useless if the person is unconscious after falling down.

The recent advancements in computer vision technology have brought together a new solution to overcome these drawbacks. One of the main advantages of visual-based fall detection is that such system does not require a person to wear anything, and it is less intrusive compared to the wearable sensor. Moreover, computer vision system provides more information on the behavior of a person compared with the normal wearable sensors. With this, visual-based home monitoring system is able to give information on falls and also other activities of daily living behaviors which are useful for home healthcare monitoring, such as medication intake, mealtime, and sleep duration.

This paper is organized as follows. Section 2 presents topics related to visual-based fall detection techniques with special emphasis on techniques that are based on human shape variation. Section 3 discusses the proposed simple visual-based fall detection technique, in which a number of essential points are used to model the human shape and the methodology to detect falls by analyzing the point features. Section 4 discusses the performance of the proposed techniques and compares its performance with the conventional fall detection techniques. Finally, Sect. 5 provides a conclusion of our work and discusses some possible future research directions.

2 Related work

In recent years, due to the advancements in computer vision technology, some work has been done in visual-based fall

detection [6]. One of the main challenges for visual-based fall detection system is how to maximize the fall detection rate with minimal computational complexity. Although there are complex algorithms [8,9] that can give very high accuracy in fall detection, these techniques normally require high processing power for real-time video processing which may not be practical for real-time practical deployment.

One of the conventional methods of detecting a fall from the surveillance video is to analyze the person’s bounding box in a single image [10,11]. The bounding box method is simple and easy to implement. However, this method works effectively only when the surveillance camera is placed sideways or at the same level as the human object. The accuracy of this technique depends on the relative position of the person and the field of view of the camera and can fail due to occluding objects. Tao et al. [12] used the aspect ratio of the bounding box to detect a fall and placed two cameras at different heights in a room to test the accuracy of their system. All simulated falls were detected for the camera placed at the table while only some of the falls were detected for the camera mounted on the wall.

Some researchers mounted the surveillance camera on the wall instead of placing it at the same level as the human object to have a larger field of view and less occluding objects [13,14]. Since bounding box could not efficiently discriminate “fall-down” from “fall-like” activities under an oblique setting of camera, ellipse features were later introduced with improved results [13,14]. Rougier et al. [13] and Chen et al. [14] combined human shape analysis with other analyses, namely motion analysis and posture estimation analysis in their approaches to detect falls. In their human shape analysis, they represent the human in the video by using ellipse shape. In comparison with the bounding box method, ellipse shape-based approach in [13,14] gives a better representation of human shape and good accuracy in fall detection, but some lure activities like sitting down brutally and squatting down brutally in parallel with the camera optical axis are still detected as fall. Moreover, ellipse features alone are not sufficient to reduce the false alarm rate to an acceptable range [14]. Therefore, combination of other analysis was used to increase the specificity of the system at the expense of increased computational complexity [13,14].

To address this problem, we propose a novel visual-based fall detection technique that is based on human shape analysis. Our proposed technique represents the person in the video sequence by using three points instead of the conventional ellipse or bounding box. From the three points, two lines are formed and features extracted from these lines are used to detect a fall. The main contribution of this paper is a low computational complexity algorithm for human shape analysis to reduce the execution time required to process one frame of video while still maintaining high fall detection accuracy.

3 Our approach

Human shape is one of the simple features used by many algorithms in detecting a fall by using surveillance video. When a person falls, the human shape will change rapidly while during normal routine daily activities, the human shape will change slowly, and this is the principle used by our proposed technique. Due to the weaknesses of the bounding box and the approximate ellipse mentioned in Sect. 2 above, we chose to model the human shape by a number of essential points. Extraction of human body points from video frame is simple and less complicated, in comparison with the conventional ellipse technique. The point representation used in our approach can provide good information on the orientation and the height proportion of a person. Background subtraction method is used to detect the person in the video sequence. From the foreground detected, three points that represent different regions of a human body, namely the head, body, and legs, are computed. Based on the computed three points, features such as change of orientation, sum of the heights, and ratio of heights are then derived and used to analyze shape change of the human. Figure 1 shows the general block diagram of the proposed technique.

3.1 Human detection

Our background subtraction approach is based on median filtering method [6]. The background of the scene and the moving person is detected by finding the difference between the incoming frames with the background model. In comparison with background subtraction by using mixture of Gaussian [6], our approach of using median filtering method has lower computational complexity and provides relatively good object detection.

3.2 Our proposed three-point human shape representation

The foreground detected is represented by three different points, which are the centroids of three different regions of the foreground region, as shown in Fig. 2. The bounding box of the foreground blob is first computed, after which the bounding box of the blob is divided into three portions with the ratio of 30:40:30%, as depicted in Fig. 2. The ratio of 30:40:30% is a preliminary estimate to distinguish between the upper, mid-, and lower body parts. Let these regions be R_1 , R_2 , and R_3 . The heights, h_{R_1} , h_{R_2} , h_{R_3} , and the widths, w_{R_1} , w_{R_2} , w_{R_3} , of R_1 , R_2 , and R_3 are calculated as:

$$\begin{aligned}
 h_{Ri} &= \begin{cases} (0.4i - 0.1i^2)H & \text{if } H > W \\ H & \text{otherwise} \end{cases} \\
 W_{Ri} &= \begin{cases} W & \text{if } H > W \\ (0.4i - 0.1i^2)W & \text{otherwise} \end{cases}
 \end{aligned}
 \tag{1}$$

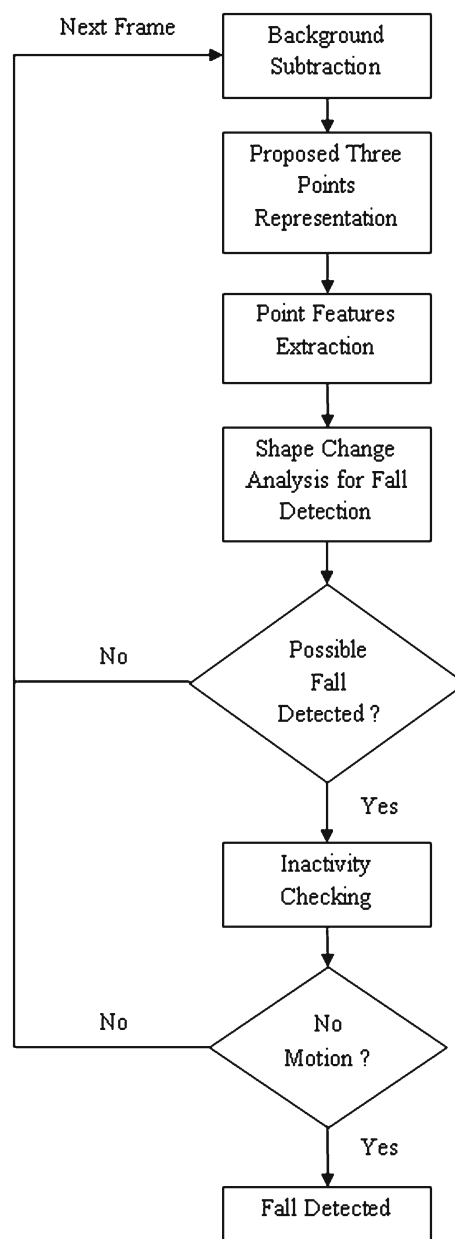


Fig. 1 General block diagram of our approach

where $i = 1, 2, 3$. H and W are the height and the width of the bounding box, respectively.

Since h_{R_1} , h_{R_3} , w_{R_1} , w_{R_3} , the starting point and the end point of the bounding box, are known, pixels in the blob that lie between these points can be used to calculate the centroids in these regions. The coordinates of the centroids are computed by:

$$g_{Rix} = \frac{1}{N_{Ri}} \sum_{l=1}^{N_{Ri}} x_l, \quad i = 1, 2, 3 \tag{2}$$

$$g_{Riy} = \frac{1}{N_{Ri}} \sum_{l=1}^{N_{Ri}} y_l, \quad i = 1, 2, 3 \tag{3}$$

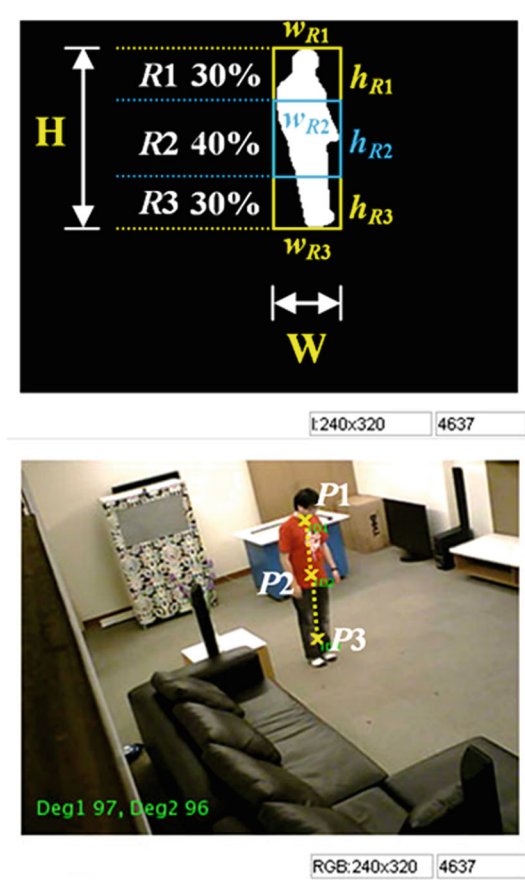


Fig. 2 Illustration of the proposed three-point human body shape representation

where N_{Ri} is the number of foreground pixels in the region Ri . The centroids are points (g_{R1x}, g_{R1y}) , (g_{R2x}, g_{R2y}) , and (g_{R3x}, g_{R3y}) for the regions $R1$, $R2$ and $R3$, respectively.

From the three centroids, we consider two lines, one from $P1$ to $P2$ and another from $P2$ to $P3$, as shown in Fig. 2. Since each line represents half portion of the foreground, any changes in the distance and the orientation of the lines can indicate a change in the shape of the person in the image. The distances and orientations of each line are then computed for shape analysis. The distances, $D1$ and $D2$, between the points are given as:

$$D1 = \sqrt{(g_{R1x} - g_{R2x})^2 + (g_{R1y} - g_{R2y})^2} \tag{4}$$

$$D2 = \sqrt{(g_{R2x} - g_{R3x})^2 + (g_{R2y} - g_{R3y})^2} \tag{5}$$

The angle between the horizontal axis x and the line formed gives the orientation of line can be computed as follows:

$$\theta_1 = \arctan \left(\frac{g_{R1y} - g_{R2y}}{g_{R1x} - g_{R2x}} \right) \tag{6}$$

$$\theta_2 = \arctan \left(\frac{g_{R2y} - g_{R3y}}{g_{R2x} - g_{R3x}} \right) \tag{7}$$

where θ_1 and θ_2 are the orientations of the line formed by $P1$ and $P2$ and the line formed by $P2$ and $P3$, respectively.

3.3 Fall recognition based on human shape analysis and inactivity period

Our approach in fall recognition is based on the fact that different changes in human posture, such as a change from standing to sitting down or a change from standing to falling, will have different changes between the upper portion and the lower portion of the human body, as shown in Fig. 3. By analyzing the shape change in these two portions of a person, we can distinguish a fall from normal daily activities. For this purpose, we compute the ratio of the distance, $p = D1/D2$, and the difference between the line orientations, θ_1 and θ_2 . Figure 4 shows the pseudocode of the fall recognition algorithm of our proposed technique.

As the shape of the upper portion and the lower portion of human body does not change much in most of the daily activities, the value of the ratio, p , will be 1 at most of the time. By computing the ratio of the distance, p , for several video sequences consisting of daily activities and simulated falls, we have Fig. 5, in which the value of the ratio will only change from value 1 to other values during a fall and some normal daily activities like squatting down, crouching down, and walking. Thus, we consider there is a possible fall if the ratio of the distance, p , suddenly changes from value 1 to another value.

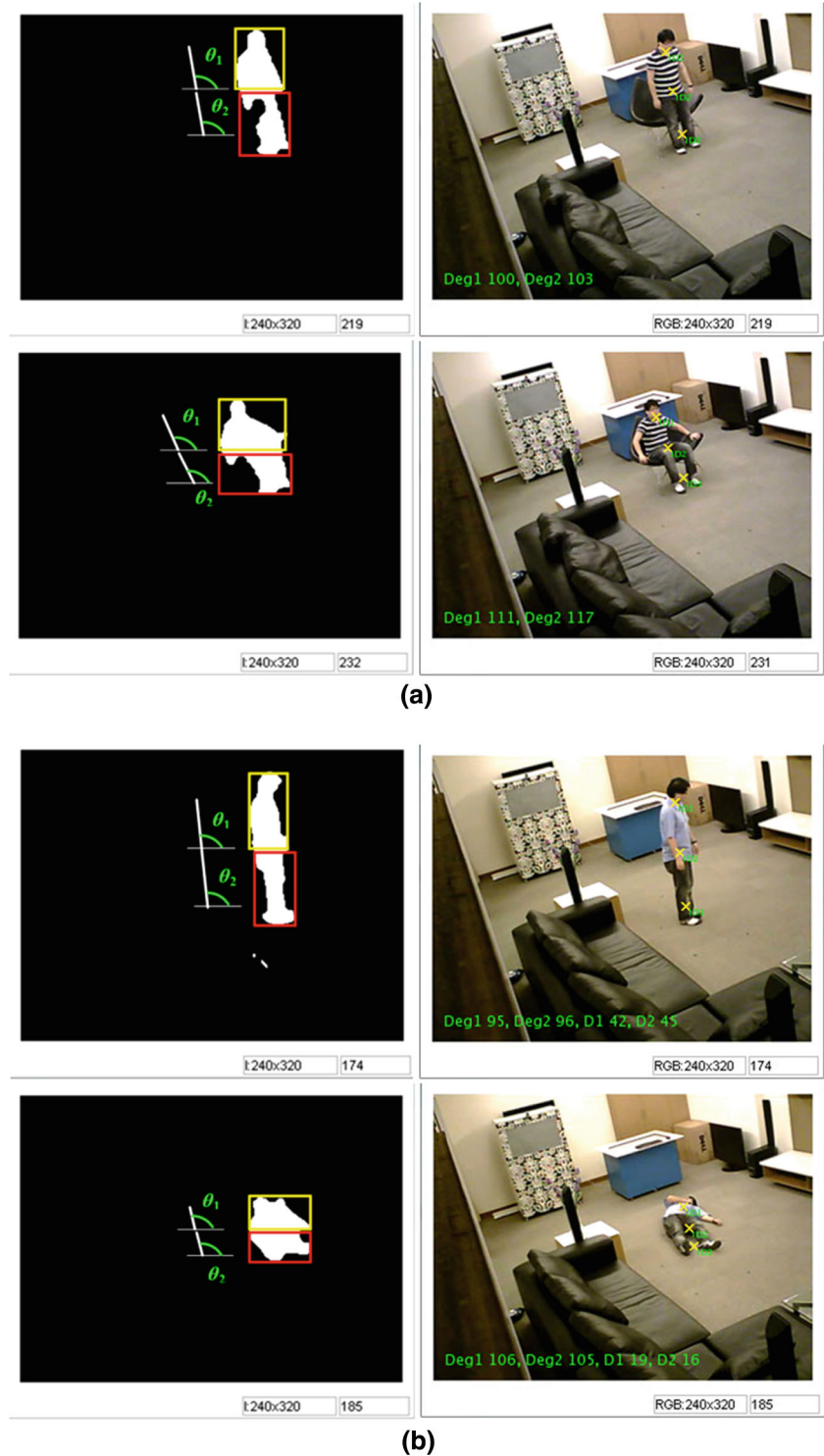
The upper and the lower parts of the human body will have similar orientation for standing and lying poses. Since the shape of a falling person will change from standing to lying, the difference between the line orientations themselves before a fall and after the fall will be small. Therefore, we check the difference between θ_1 and θ_2 for each frame. θ_1 and θ_2 are considered to be similar to each other if the difference between them is less than $10^\circ (\Delta\theta < 10^\circ)$.

First, ratio of the line distance from the previous frame, p_{t-1} , is compared with the ratio of line distance of the current frame, p_t . If there is no possible fall ($\Delta p = 0$) and the line orientations are similar, θ_1 is stored as a reference angle, θ_r , and the sum of $D1$ and $D2$ is stored as length reference, D_r . Whenever there is a possible fall ($\Delta p > 0$), we will search for line orientations, θ_1 and θ_2 , that are similar to each other at the 10th frame after the possible fall and store them as θ_{N1} and θ_{N2} , respectively. Ten frames are used as a time interval for fast movement in our test videos. Other number of frames can be set to cope with frame rate of the video sequences. We then compute the difference between each of the most recent stored line orientations with the reference angle, as follows:

$$\theta_{D1} = |\theta_{N1} - \theta_r| \tag{8}$$

$$\theta_{D2} = |\theta_{N2} - \theta_r| \tag{9}$$

Fig. 3 Example of change of orientations and shape dimensions at the upper portion and lower portion of a person during posture change: **a** from standing to sitting down, **b** from standing to falling down



where θ_{D1} is the orientation difference between θ_{N1} and θ_r while θ_{D2} is the orientation difference between θ_{N2} and θ_r . To overcome the problem of mapping two portions of the human body before a fall and after a fall, the mean of these two orientation differences, μ_θ , is computed. We then consider a fall detected if μ_θ is more than 30° .

However, there are falls where the value of μ_θ can be less than or equal to 30° . Therefore, under this condition, we check the difference between the total line length at the 10th frame after a possible fall and the length reference, D_r . Based on our observations, the height of the person will reduce drastically during a fall in the field of view of the camera, as


```

IF difference of the ratio of distance,  $\Delta p$ , is greater than one
  IF frame count hasn't start, frame count = 0
  SET frame count = 1
ENDIF
ENDIF

COMPUTE the angle difference between  $\theta_1$  and  $\theta_2$ 

IF angle difference is less than 10 degrees
   $\theta_1$  and  $\theta_2$  are similar to each other
ELSE
   $\theta_1$  and  $\theta_2$  are not similar to each other
ENDIF

IF  $\theta_1$  and  $\theta_2$  are similar
  IF frame count = 0
    SET  $\theta_r$  equals to  $\theta_1$ 
    SET  $D_r$  equals to sum of  $D1$  and  $D2$ 
  ELSE
    SET  $\theta_{N1} = \theta_1$ 
    SET  $\theta_{N2} = \theta_2$ 
    IF frame count = 10
      COMPUTE  $\theta_{D1} = |\theta_{N1} - \theta_r|$ 
      COMPUTE  $\theta_{D2} = |\theta_{N2} - \theta_r|$ 
      COMPUTE  $\mu_\theta = \text{average of } \theta_{D1} \text{ and } \theta_{D2}$ 
      IF  $\mu_\theta > 30$  degrees
        SET fall status to true
      ELSE
        COMPUTE  $D_{diff} = |D_r - (D1 + D2)|$ 
        IF  $D_{diff} > 0.40 * D_r$ 
          SET fall status to true
        ELSE
          SET fall status to false
        ENDIF
      ENDIF
    ENDIF
  ENDIF
ELSE
  SET fall status to false
ENDIF

IF fall status is true
  CALL check inactivity function
ELSE
  RETURN
END

IF frame count = 10
  SET frame count = 0
ELSEIF frame count  $\neq 0$ 
  INCREMENT frame count value by one
ENDIF

```

Fig. 4 Pseudocode of the shape analysis algorithm of our proposed technique

depicted in Fig. 6. The change in sum of the length of the lines after a possible fall, D_{diff} , is given by:

$$D_{diff} = |D_r - (D1 + D2)| \quad (10)$$

A fall is detected if D_{diff} is larger than 40% of the length reference, $0.40 * (D_r)$ pixels. If the line orientations, θ_1 and θ_2 , are not similar to each other at the 10th frame after the possible fall, the system considers it as no fall is detected. Figure 7 shows some examples of daily activities and simulated falls with their corresponding changes in p , θ_1 and θ_2 .

A fall will end with an inactivity period if the person is immobilized or unconscious after the fall. The last verifica-

tion of our approach is to check whether there is any movement of the person after a possible fall. A fall is confirmed if the following condition is fulfilled:

1. Change in distance moved by the centroid, $P2$, is smaller or equal to 5 pixels for 5 s. For testing purpose, 5 s was chosen to be the duration of the inactivity period in our approach. A longer duration of the inactivity period can be used to ensure the person is completely unconscious after a fall.

4 Experiment results

Our system was implemented using MATLAB on a PC using Intel Core i3 2.13 GHz CPU with 4 GB RAM. All test video data were acquired from an uncalibrated IP camera (Dlink DCS-920) through Wi-Fi connection in MJPEG format at a resolution of 320×240 .

Our test video data consist of video sequences of 30 daily activities such as walking, sitting down, crouching down, and squatting down, and 21 simulated falls such as backward falls, forward falls, sideways falls, and falls due to loss of balance. Our fall video data set is available at <http://foe.mmu.edu.my/digitalhome/FallVideo.zip>. Figure 8 shows that our proposed technique is able to track the human correctly in the presence of other moving objects by setting a minimum area threshold to differentiate human from other moving objects, for example, pets, with the fact that the size of a normal adult is always larger than the sizes of the pets.

Table 1 shows the experiment results of our proposed fall detection technique. Two fall incidents were not detected because the human body of the person was in a straight line during these falls, as shown in Fig. 9. Thus, the ratio of the distances, p , remained as 1 ($\Delta p = 0$), and the system considered there is no possible fall. On the other hand, two brutally crouch-down activities were detected as fall because of the sudden change in the ratio of the distances, p , from 1 to 2, and due to the change in the mean of orientation difference is greater than the predefined threshold value ($\mu_\theta > 30^\circ$). Overall, our proposed system can achieve high accuracy in fall detection with a detection accuracy of 90.5% and false alarm rate of 6.7%. The operating characteristics of the proposed technique are tabulated in Table 2. The threshold values for mean orientation difference, μ_θ , and post-fall total length difference, D_{diff} , from Sect. 3.3 above are defined based on the result in Table 2. Instead of 40° or 50° , 30° is chosen as the threshold value for μ_θ because a smaller angle difference gives a bigger chance of detecting falls which are almost parallel to the camera optical axis.

We compare our proposed technique with the bounding box ratio analysis approach [10], ellipse shape analy-

Fig. 5 Example of change in the ratio of the distances, p , during: **a** falling, **b** walking, and **c** crouching-down event

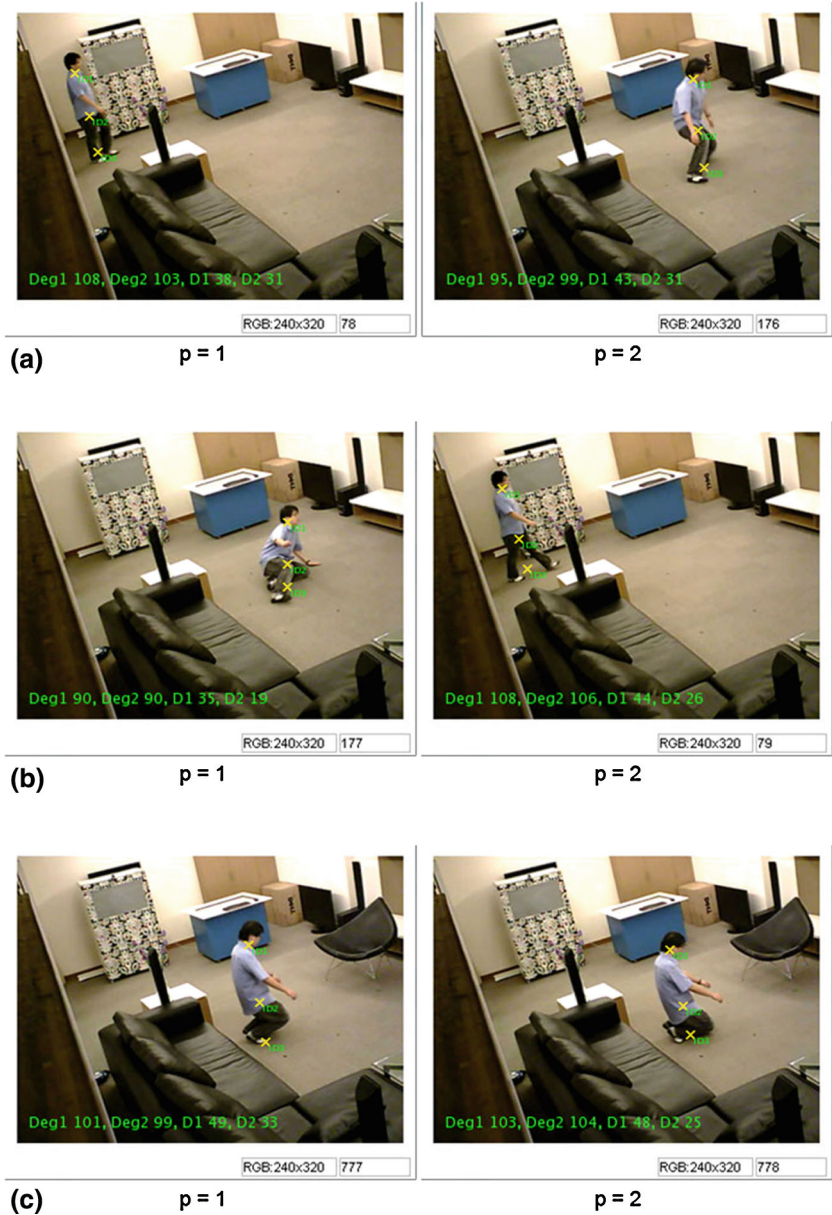
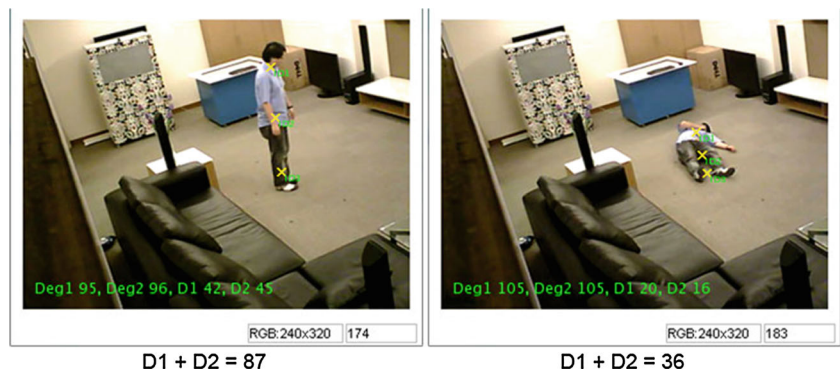


Fig. 6 Changes in the total distance of the human body during some fall events. Example of the change in the total distance of the human body during a fall which is parallel to the camera optical axis



sis approach [13], and Chen’s approach [14] in terms of time complexity. The time complexity of our proposed technique is similar to the time complexity of the bounding box

ratio analysis approach [10] and the ellipse shape analysis approach [13], which is $O(n)$ complexity where n is the pixel resolution of one video frame. The time complexity of Chen’s

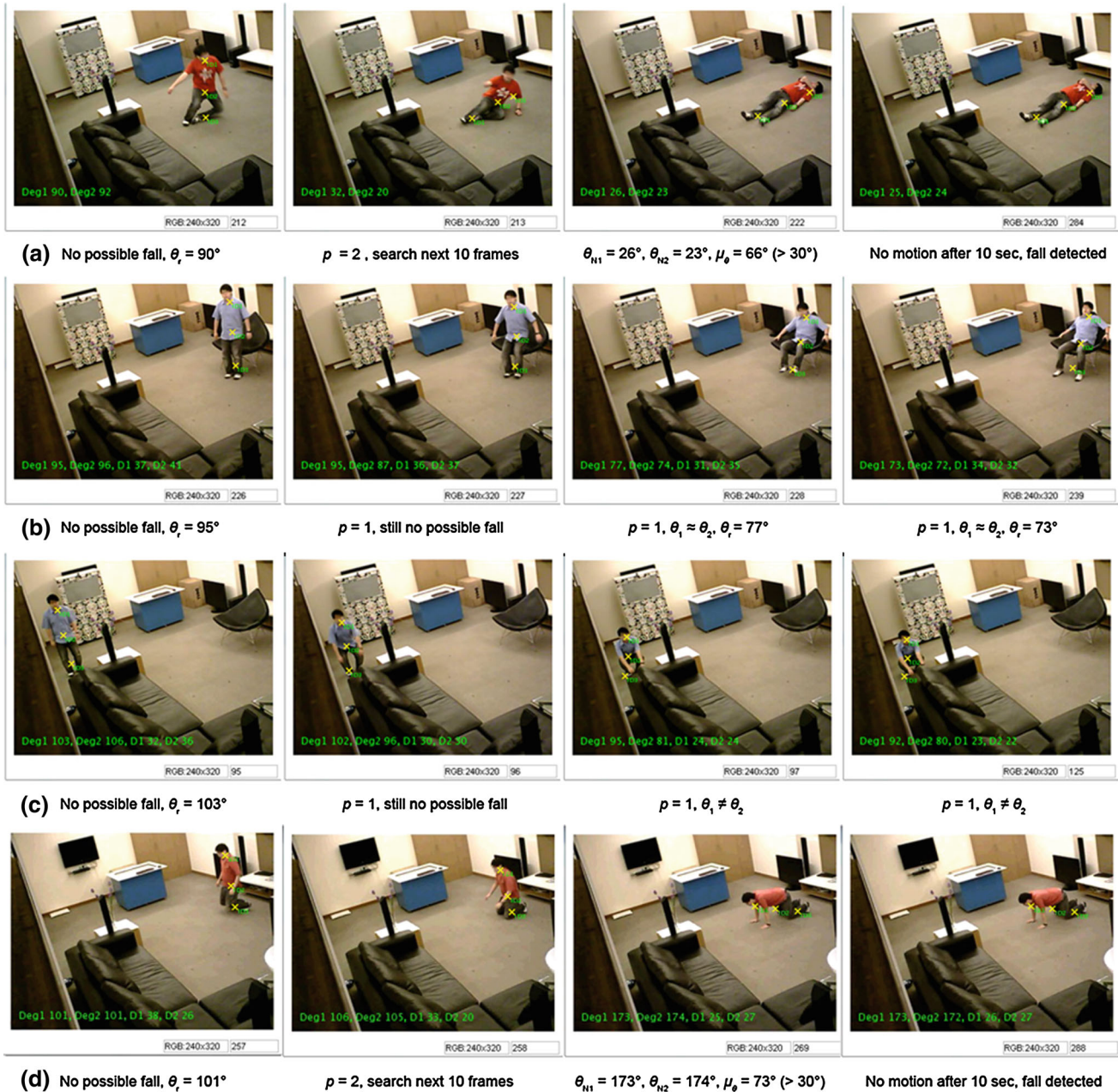


Fig. 7 Examples of daily activities and simulated fall with their corresponding changes in p , θ_1 , and θ_2 . **a** Example of detecting a fall where the difference between the line orientations before the fall and after the fall is greater than 10° , followed by no movement of the person after 5 s. **b** No possible fall is detected for sit-down activity as the ratio of

the distances is still 1 throughout the activity. **c** Similar case with **(b)** where no possible fall is detected for squat-down activity. **d** Example of error detection where a fall is detected due to the change in the mean of orientation difference is greater than the predefined threshold value during crouch-down activity

approach [14] is $O(n \log n)$. Table 3 compares the total number of primitive operations required to extract the features for shape analysis in one video frame for those approaches that have the order of n time complexity, $O(n)$. Other than comparing the time complexity of these techniques, Table 4 compares our proposed technique with other four human fall detection approaches in terms of fall detection rate, false

alarm rate, and execution time. Results for the bounding box ratio analysis approach [10] and the ellipse shape analysis approach [13] in Table 4 were obtained through simulation from the same video data used in testing our proposed technique, while the results for Chen's approach [14] and Bio-mechanics approach [7] were obtained from their original paper.

Fig. 8 Example of the correct tracking of human in the presence of other moving object during: **a** walking and **b** falling. In this case, the moving robot on the ground can be treated as a pet

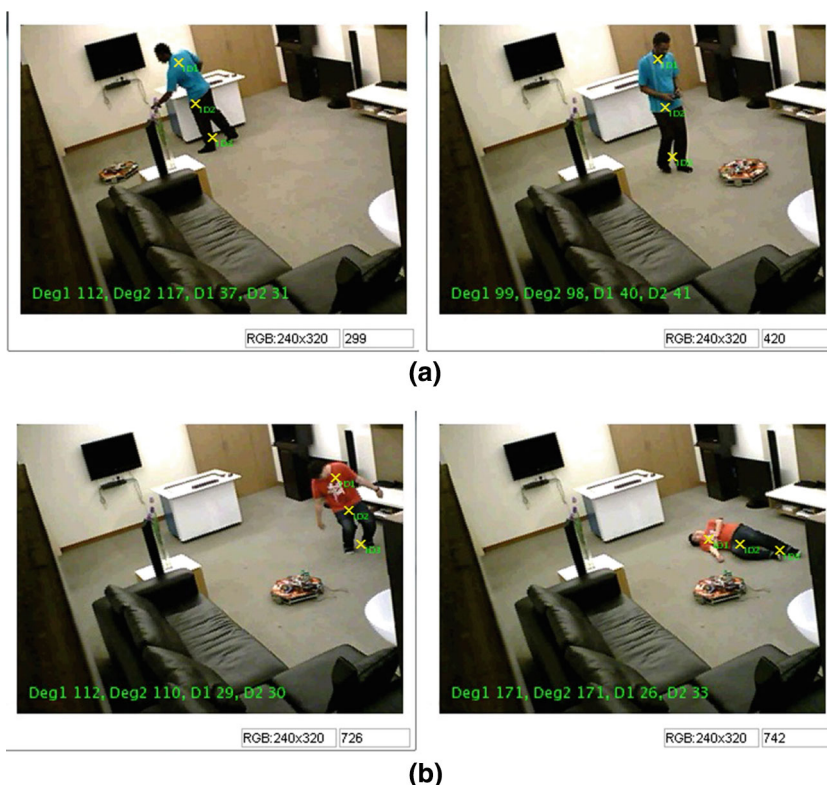


Table 1 Fall detection results of our proposed technique

Incidents	Falls detected	Falls not detected	Accuracy
Falls	19	2	Fall detection 90.5 %
Daily activities	2	29	False alarm 6.7 %

It can be observed from the time complexity of each approach and Table 3 that our proposed technique has lower computational complexity compared to Chen’s approach [14], which has high accuracy in fall detection and low false alarm rate due to the combination of two different analyses used, but having nearly the same computational complexity as the bounding box ratio analysis approach [10] and ellipse

shape analysis approach [13]. Despite having the same time complexity with the two shape analysis approaches [10, 13], our proposed method, as shown in Table 4, can achieve better performance in terms of detecting falls and distinguishing a fall from normal daily activities. As compared to Chen’s approach [14], our proposed technique results in similar performance in terms of fall detection rate and false alarm rate, but with a lower computational cost. Table 4 also summarizes that the accuracy of using biomechanics approach [7] to detect typical falls still surpasses the accuracy given by visual-based human fall detection approaches. Furthermore, biomechanics approach does not have the issues of occlusion and varying illumination. However, visual-based fall detection system can be treated as the complement to the existing



Fig. 9 Example of the no changes in the ratio of the distances ($\Delta p = 0$) during a fall

Table 2 Operating characteristics of our proposed technique

$\mu_{\theta} >$	$D_{\text{diff}} > 20\%$ of D_r		$D_{\text{diff}} > 40\%$ of D_r		$D_{\text{diff}} > 60\%$ of D_r	
	True-positive rate (%)	False-positive rate (%)	True-positive rate (%)	False-positive rate (%)	True-positive rate (%)	False-positive rate (%)
10°	90.5	10.0	90.5	10.0	81.0	10.0
20°	90.5	10.0	90.5	10.0	76.2	10.0
30°	90.5	10.0	90.5	6.7	76.2	6.7
40°	90.5	10.0	90.5	6.7	76.2	6.7
50°	90.5	10.0	90.5	6.7	76.2	6.7

Table 3 Comparison of the total number of primitive operations executed for approaches having $O(n)$ time complexity

Approaches	Number of primitive operations per frame
Our proposed technique	$8n + 64$
Bounding box ratio analysis approach [10]	$5n + 24$
Ellipse shape analysis approach [13]	$8n + 67$

n pixel resolution of one video frame

Table 4 Comparison of our proposed technique with four human fall detection approaches in terms of fall detection rate, false alarm rate, and execution time

Metrics	Our proposed technique	Bounding box ratio analysis approach [10]	Ellipse shape analysis approach [13]	^a Chen's approach [14]	^a Biomechanics approach [7]
Fall detection rate (%)	90.5	66.0	85.7	90.9	100.0
False alarm rate (%)	6.7	26.7	20.0	6.25	0.0
Execution time per frame (s)	0.19	0.12	0.18	4.21	–

^a Results provided by original authors

fall alert products to overcome the weaknesses that fall alert products have, which is the elderly might forget to wear the fall detection sensor.

5 Conclusions

In this work, we presented an improved visual-based fall detection technique with high detection accuracy. Our proposed technique simplifies the ways to represent human shape by using three centroids of different regions of the human body instead of the conventional bounding box or an ellipse. This method is able to give information on the changes in the upper portion and the lower portion of the human body. Experiment results indicate that our proposed technique can achieve high accuracy for human fall detection in real-time indoor video sequences.

In our future work, we will look into ways to improve the accuracy of our proposed technique in varying lighting condition and methods to cope with occlusion. We will explore the possibility of reducing the false alarm rate of our system

by adding low computational head tracking algorithm in our proposed technique.

Acknowledgments This work was supported in part by Telekom Malaysia Research and Development (TM R&D) research grant.

Conflict of interest The authors declare that they have no competing interests.

References

1. Hausdorff, J.M., Rios, D.A., Edelber, H.K.: Gait variability and fall risk in community-living older adults: a 1-year prospective study. *Arch. Phys. Med. Rehabil.* **82**(8), 1050–1056 (2001)
2. Population Statistics in Malaysia. Department of Statistic Malaysia [Online]. Available: <http://www.statistics.gov.my> (2010)
3. Hashim, A.: Overview of Malaysia's Integrated Telehealth Project. *The International Medical Journal*. [Online]. Available: <http://www.eimjm.com/Vol2-No1/Vol2-No1-I4.htm> (2003)
4. World Population Ageing. United Nations, New York [Online]: Available: <http://www.un.org/esa/population/publications/WPA2009/WPA2009-report.pdf> (2009)
5. Falls among Older Adults: An Overview. Web-based Injury Statistics Query and Reporting System (Centers for Disease

- Control and Prevention, National Center for Injury Prevention and Control). [Online]. Available: <http://www.cdc.gov/HomeandRecreationalSafety/Falls/adultfalls.html>. Accessed 11 March 2011
6. Willems, J., Debard, G., Bonroy, B., Vanrumste, B., Goedemé, T.: How to detect human fall in video? An overview. In: International Conference on Positioning and Context-Awareness, Antwerp Belgium, May 2009
 7. Nguyen, T.-T., Cho, M.-C., Lee, T.-S.: Automatic fall detection using wearable biomedical signal measurement terminal. In: Proceedings of 31st Annual International Conference of the IEEE EMBS, pp. 5203–5206 (2009)
 8. Rougier, C., Meunier, J., St-Arnaud, A., Rousseau, J.: Robust video surveillance for fall detection based on human shape deformation. *IEEE Trans Circuits Syst. Video Technol.* **21**(5), 611–622 (2011)
 9. Cucchiara, R., Prati, A., Vezzani, R.: A multi-camera vision system for fall detection and alarm generation. *Expert Syst J* **24**(5), 334–345 (2007)
 10. Williams, A., Ganesan, D., Hanson, A.: Aging in place: fall detection and localization in a distributed smart camera network. In: Proceedings of the 15th international conference on Multimedia, pp. 892–901 (2007)
 11. Vishwakarma, V., Mandal, C., Sural, S.: Automatic detection of human fall in video. *Lect. Notes Comput. Sci. Patt. Recogn. Mach. Intell.* **4815**, 616–623 (2007)
 12. Tao, J., Turjo, M., Wong, M. F., Wang, M., Tan, Y. P.: Fall incidents detection for intelligent video surveillance. In: Proceedings of IEEE International Conference on Communication and Signal Processing, pp. 1590–1594 (2005)
 13. Rougier, C., Meunier, J., St-Arnaud, A., Rousseau, J.: Fall detection from human shape and motion history using video surveillance. *Proc. 21st Int. Conf. AINAW* **2**, 875–880 (2007)
 14. Chen, Y.T., Lin, Y.C., Fang, W.H.: A hybrid human fall detection scheme. In: Proceedings of 2010 IEEE 17th International Conference on Image Processing, pp. 3485–3488 (2010)